MODEL PREDICTIVE CONTROL DESIGN OF DC-DC CONVERTER FOR ELECTRIC VEHICLE CHARGER APPLICATION

École Centrale de Nantes

Juan Carlos Escalante Díaz del Campo

Bramantio Yuwono

January 2023

Table of Contents

1. Introduction

As demand for electric vehicles has been in the rising trend, the necessity for electric vehicle charging stations has also increased in the past years [1]. The growth in the number of EV charging stations plays the major part of tackling the main barriers of EV adoption: range anxiety. More charging stations deployed on the road can facilitate longer journeys, enable longer trips and encourage consumers to purchase an EV.

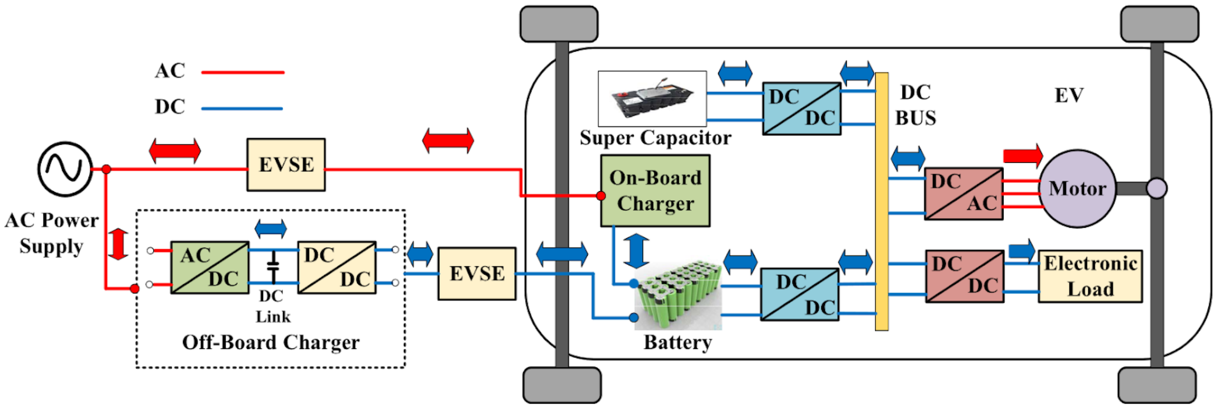

Figure 1. EV charging system including off-board and on-board charger [2]

There are two architectures of EV charging currently in the market, on-board charger and off-board charger, as shown in *Figure 1*. On-board charger performs the AC-DC conversion inside the EV, while off-board charger converts AC to DC outside the vehicle and allows more space for components and cooling. Because of this reason, off-board charger can provide faster charging and higher charging power (50kW - 350kW) compared to on-board charger (1.44kW - 19.2kW) [2]. Off-board charger consists of two parts, a rectifier to convert AC voltage from the grid to DC voltage and a DC-DC converter to provide the voltage level required for the battery. Due to possibilities of a drop or rise in the voltage grid and increasing or decreasing battery internal resistance related to its state-of-health(SOH), a robust DC-DC converter control method is imperative to ensure the charger performance. Model predictive control(MPC) has emerged as one of many promising control techniques for converter application, thanks to technological advancements in microprocessors and microcontrollers as it requires a large computational burden. MPC presents several advantages: simple to apply in multivariable systems, able to provide a fast dynamic response, can allow nonlinearities and constraints [3].

This work provides the simulation of MPC control for DC-DC buck converter to evaluate the robustness of MPC control strategy when disturbances on converter's input voltage and load resistances are applied. After this Introduction section, the modelling of DC-DC buck converter and its implementation on MATLAB/Simulink is explained. Afterwards, the explanation of MPC is discussed in the third section. Then, the fourth section will present the simulation result. Lastly, the conclusion of this work is elaborated in the last section.

2. DC-DC Buck Converter Modelling

2.1. Basic Principle

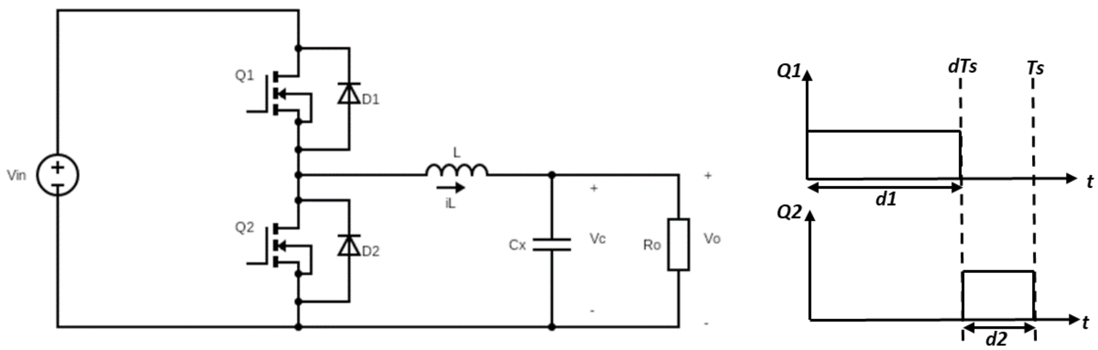

Figure 2. (a) Buck Converter Topology [4], (b) Switching Operation

The circuit of the buck converter is shown in *Figure 2(a)*. Since the voltage level given by the rectifier in the off-board EV charger is mostly higher than the level of the battery [2], a buck converter is needed to regulate voltage to the required level in high efficiency. The basic operation of the buck converter is determined by the switching operation between *Q1* and *Q2* switches. During *d1* operation, *Q1* is on and *Q2* is off, allowing the input voltage to charge the inductor and the capacitor. On the other hand, *Q1* is off and *Q2* is on in the *d2* operation, enabling a charged inductor and capacitor to supply current and voltage to the load. Therefore, the output voltage level can be obtained through controlling the duty cycle *d* or the proportion of *d1* operation in one sample time *Ts* (hence *d2 = 1 - d*). Its value ranges from 0 to 1.

The relation between input voltage, duty cycle and output voltage of the buck converter in equilibrium is shown in the below equation.

$$V_o = d * V_{in} \tag{1}$$

2.2. Mathematical Analysis

To perform mathematical analysis of a buck converter, it can be done by splitting up the analysis into two parts: during *d1* operation and *d2* operation.

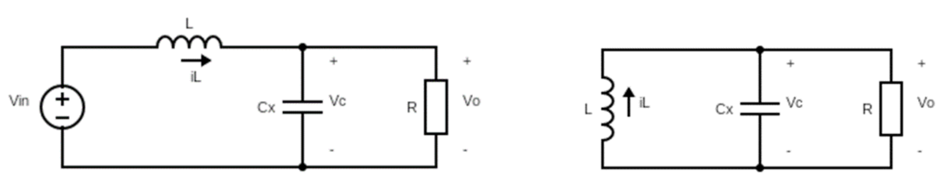

Figure 3. (a) Buck Converter Equivalent Circuit during d1, (b) Buck Converter Equivalent Circuit during d2

During *d1* operation, the equivalent circuit of the buck converter is shown in *Figure 3(a)*, while *Figure 3(b)* shows the equivalent circuit in the *d2* operation. Analysis is performed by applying Kirchoff voltage law on inductor's voltage and Kirchoff current law on capacitor's current in circuit for both operations.

For *d1* operation (*Q1* on and *Q2* off):

- Inductor current equation

$$V_{in} = v_L + v_C \tag{2}$$

$$V_{in} = L\frac{di_L}{dt} + v_C \tag{3}$$

$$\dot{i_{L,d1}} = \frac{V_{in}}{L} - \frac{v_C}{L} \tag{4}$$

- Capacitor voltage equation

$$i_L = C_x\frac{dv_C}{dt} + \frac{v_C}{R_o} \tag{5}$$

$$i_L = C_x\frac{dv_C}{dt} + \frac{v_C}{R_o} \tag{6}$$

$$\dot{v_{C,d1}} = \frac{i_L}{C_x} - \frac{v_c}{R_o C_x} \tag{7}$$

For *d2* operation (*Q1* off and *Q2* on):

- Inductor current equation

$$v_L = -v_C \tag{8}$$

$$L\frac{di_L}{dt} = -v_C \tag{9}$$

$$\dot{i_{L,d2}} = -\frac{v_C}{L} \tag{10}$$

- Capacitor voltage equation

$$i_L = C_x\frac{dv_C}{dt} + \frac{v_C}{R_o} \tag{11}$$

$$i_L = C_x\frac{dv_C}{dt} + \frac{v_C}{R_o} \tag{12}$$

$$\dot{v_{C,d2}} = \frac{i_L}{C_x} - \frac{v_c}{R_o C_x} \tag{13}$$

After defining the inductor current equation and the capacitor voltage equation, we can combine (4) with (10) and (7) with (13) by multiplying its term with its respective operation time proportion in a one time sample Ts (*d1 = d* and *d2 = 1-d*). It will give results as shown in (14) and (15).

$$\dot{i_L} = \dot{i_{L,d1}} + \dot{i_{L,d2}} = \frac{1}{L}\left[(V_{in} - v_c)d + (-v_C)(1-d)\right] = \frac{V_{in}}{L}d - \frac{v_C}{L} \tag{14}$$

$$\dot{v_C} = \dot{v_{C,d1}} + \dot{v_{C,d2}} = \frac{1}{C_x}\left[\left(i_L - \frac{v_C}{R_o}\right)d + \left(i_L - \frac{v_C}{R_o}\right)(1-d)\right] = \frac{i_L}{C_x} - \frac{v_c}{R_o C_x} \tag{15}$$

2.3. State-space Representation

From (14) and (15), the model can be represented in the state space by setting $x = \left[i_L \; v_C\right]^T$, $u = d$, and $y = v_o = v_c$. Hence, the buck converter model in state is described as:

$$\dot{x} = \begin{bmatrix} \dot{i_L} \\ \dot{v_C} \end{bmatrix} = \begin{bmatrix} 0 & -\frac{1}{L} \\ \frac{1}{C_x} & -\frac{1}{R_o C_x} \end{bmatrix} \begin{bmatrix} i_L \\ v_C \end{bmatrix} + \begin{bmatrix} \frac{V_{in}}{L} \\ 0 \end{bmatrix} d$$

$$y = v_o = \begin{bmatrix} 0 & 1 \end{bmatrix} \begin{bmatrix} i_L \\ v_C \end{bmatrix} \tag{16}$$

with

$$A = \begin{bmatrix} 0 & -\frac{1}{L} \\ \frac{1}{C_x} & -\frac{1}{R_o C_x} \end{bmatrix}, \; B = \begin{bmatrix} \frac{V_{in}}{L} \\ 0 \end{bmatrix}, \; C = \begin{bmatrix} 0 & 1 \end{bmatrix}, and\ D = 0 \tag{17}$$

This state-space representation of the buck converter is utilised in the MPC controller for the calculation of prediction model. The model with the state-space representation fed to the MPC controller is an ideal model of the buck converter and does not include the effect of disturbances on the input voltage *Vin* and the load resistance *Ro*. To be able to apply the disturbances during the simulation, the buck converter plant model that takes these disturbances into account is built separately from the state-space representation.

2.4. DC-DC Buck Converter Plant Implementation

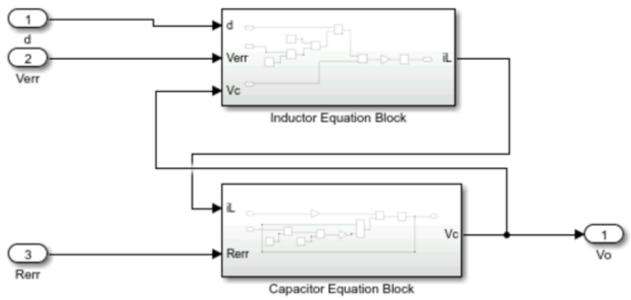

Figure 4. Buck Converter Plant Model with Disturbances Implementation Neglecting the Switching Operation

To observe the effect of disturbances on input voltage *Vin* and load resistance *Ro*, it is required to build a buck converter that can manipulate the *Vin* and *Ro* values in specific time on MATLAB/Simulink. The built model implements the inductor equation shown in (14) and the capacitor equation shown in (15) with input *d* and output voltage *Vo*. However, input *Verr* and *Rerr* is added to the model to accommodate the disturbances simulation, where *Verr* is the deviation of *Vin* from its rated value in % and *Rerr* is the deviation of *Ro* from its rated value in %. In this model however, it still neglects the switching operation and utilises the *d* value into the model instead.

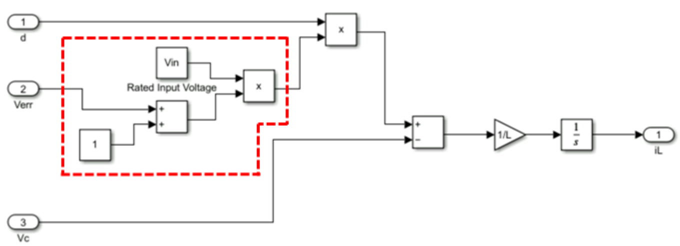

Figure 5. Inductor Equation Implementation with Neglecting the Switching Operation

Figure 5 shows the implementation of the inductor equation (14) with incorporating *Verr* into the model as shown in the red dashed line. *Verr* is implemented so it can manipulate the input voltage value *Vin* with $V_{in} = V_{in,rated} * (1 + Verr)$.

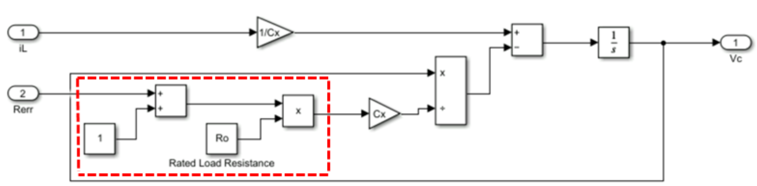

Figure 6. Capacitor Equation Implementation

The same method is used for the implementation of the capacitor equation shown in *Figure 6*. *Rerr* is implemented so it can manipulate the load resistance value *Ro* with $R_o = R_{o,rated} * (1 + Rerr)$ as shown in the red dashed line of *Figure 6*.

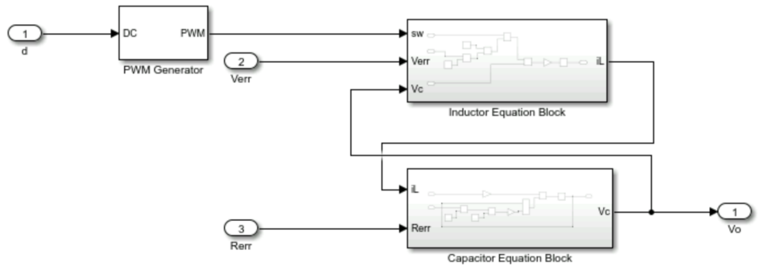

Figure 7. Buck Converter Plant Model with the Disturbances Implementation and the Switching Operation

For implementing the switching operation into the plant block, input *d* is fed into the PWM generator to generate PWM signal instead of using it in the inductor equation. This PWM generator generates 1 and 0 signals with duty cycle set in *d*. The switching signal is given to the inductor equation block as an input. The implementation of the capacitor equation block is the same to *Figure 6* since the capacitor equations for *d1* operation (7) and for *d2* operation (13) are identical.

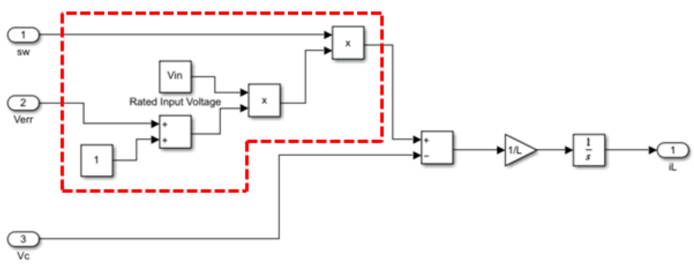

Figure 8. Inductor Equation Implementation with the Switching Operation

As seen in (4) and (10), the difference between capacitor equation for *d1* and *d2* only lies in term $\frac{V_{in}}{L}$ which only exists in the capacitor equation for *d1* and does not exist during *d2* operation. Because the PWM signal is set (*sw* = 1) only during *d1*, the switching operation can be achieved by multiplying the PWM signal *sw* with the input voltage term *Vin*.

Parameters	Values	Remarks
L	400e-6	Inductor inductance (henry)
Cx	100e-6	Capacitor capacitance (farad)
Ro	50	Rated load resistance (ohm)
Vin	400	Input voltage (volt)
Vout	350	Desired output voltage (volt)

Table 1. Buck Converter Parameters

The parameter set for our simulation in this work is shown in the table above. The input and output voltage values correspond to the value of typical rectifier output voltage and the battery voltage of Renault Zoe R110 ZE50 respectively [2]. To check the validity of the designed buck converter plant block, the step function to $d = \frac{V_{out}}{V_{in}} = \frac{350}{400} = 0.875$ at $t = 1$ and $Verr, Rerr = 0$ (without disturbances) is fed to the plant as shown in *Figure 9*.

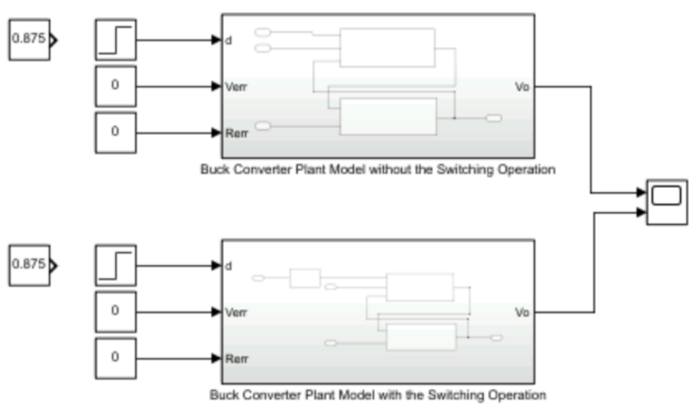

Figure 9. Simulation of the Buck Converter Plant Blocks

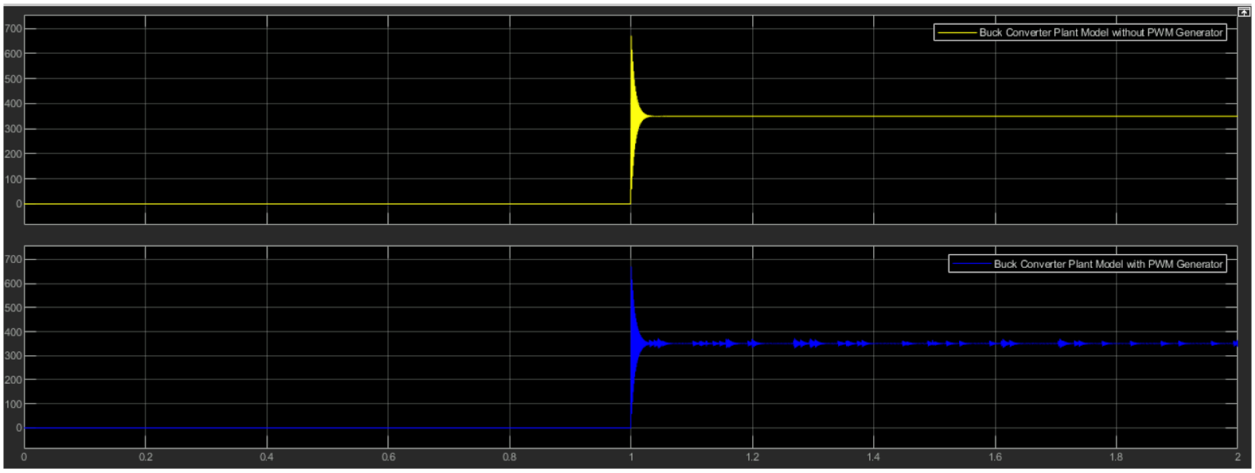

Figure 10. Step Function Response of Buck Converter Plants without switching operation(top) and with switching operation(down)

From the figure above, it can be concluded that the designed buck converter behaves as expected. After the duty cycle value is set to 0.875, the output value reaches the desired value (350V). However, it can be seen that there are very high ripples (around 300Vpp) at t=1 that can harm the converter. For the plant with the switching operation implementation, the output voltage value has ripples caused by the switching even after the output voltage reaches 350. How well the MPC controller can filter out these ripples will be the main focus also in this work.

3. Model Predictive Control

With the increasing demand of AC-DC and DC-DC charging stations, alongside with the different levels of speed for charging, the need for control techniques to make the power converters more efficient, optimal and feasible have arisen. On this investigation we focus on a Control technique that has been used for over 15 years, which is called Model Predictive Control (MPC). This type of control appeared in the industry as an effective control technique that could operate with multivariable constrained dynamics or model, our model for "DC-DC Buck Converter" is a linear model which uses the input u(t) as the duty cycle and the output then is the Voltage, so in our case, the MPC only takes one manipulated Variable which is the duty cycle, and one Input for the MPC which is the Measured Output Voltage.

MPC is based on a repeated real-time optimization of a mathematical system model [6]. Based on this system model, the MPC predicts the future system behaviour considering it in the optimization that determines the optimal trajectory of the manipulated variable u, *Figure 11*. Thus, MPC comes with an intuitive parameterization through adjusting a process model at the cost of a higher computational effort than classical controllers [5].

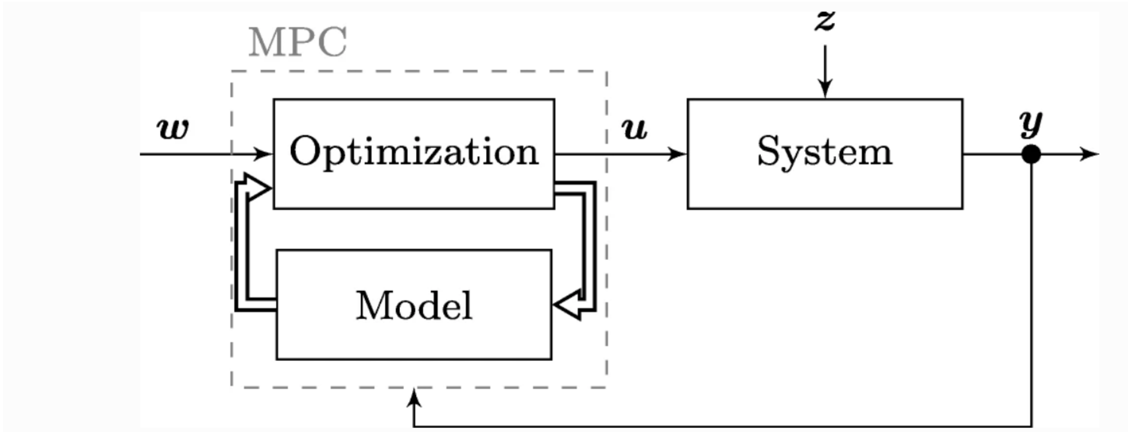

Figure 11. Simplified block diagram of an MPC-based control loop.

The anticipating behaviour and the fact that it can consider hard constraints makes the method so valuable for controlling real systems. Aligned with the rise of computational power and as models of complex processes become more and more available for all kinds of different systems, MPC now enables for the control of systems that were previously unthinkable [5]. One cannot define MPC as an explicit control law, instead MPC is a model-based optimization which determines the control law by itself.

As we stated, MPC isn't a control method by itself, instead is a synergic combination of advanced control methods, which takes into account the model of a system to predict the future behaviour and then select the optimal output of the mpc and input to the plant u, by solving a constrained optimization problem. In our case, the cost function is formulated by the MATLAB MPC designer in such a way that the plant or "system" output y tracks a given reference r for a given prediction horizon.

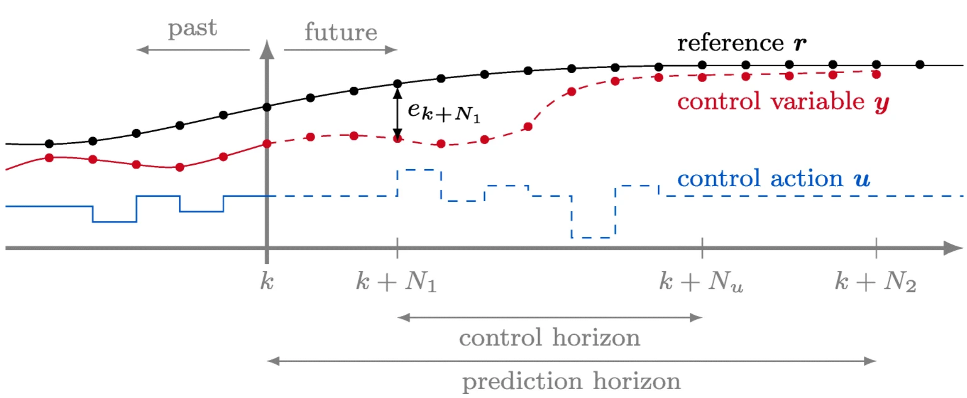

Figure 12. Function principle of a model-based predictive with horizons N1, N2, Nu (in accordance to [7])

The prediction horizon $N2$ must be long enough to represent the effect of a change in the manipulated variable u on the control variable y. Delays can be considered by the lower prediction horizon $N1$ or by incorporating them into the system model. Often, the latter is more intuitive and the lower prediction horizon is set to $N1 = 1$ to account for the computation time (hence the computation is conducted in one time step, the solution u is implemented not before the next time step) [5].

Assuming an arbitrary system:

$$\boldsymbol{x}(\boldsymbol{k}+1) \quad = \quad \boldsymbol{f}(\boldsymbol{x}(\boldsymbol{k}), \boldsymbol{u}(\boldsymbol{k})), \quad \boldsymbol{y}(\boldsymbol{k}) \quad = \quad \boldsymbol{h}(\boldsymbol{x}(\boldsymbol{k})). \tag{18}$$

MPC minimises a user-defined cost function J, Eq. 19, e.g. the tracking error between the reference vector r and the model output y, Eq. 19 [5]:

$$\min_{\boldsymbol{u}} \quad J\left(\boldsymbol{x}(\boldsymbol{k}), \boldsymbol{u}(\cdot)\right) \quad \longrightarrow \quad \min_{\boldsymbol{u}} \quad \sum_{i=N_1}^{N_2} \|\boldsymbol{r}(\boldsymbol{k}+i \mid \boldsymbol{k}) - \boldsymbol{y}(\boldsymbol{k}+i \mid \boldsymbol{k})\| \tag{19}$$

$$\begin{aligned} \text{s.t.} \qquad & \boldsymbol{u}_{lb} \leq \boldsymbol{u}(\boldsymbol{k}+j \mid \boldsymbol{k}) \leq \boldsymbol{u}_{ub} \\ & \boldsymbol{y}_{lb} \leq \boldsymbol{y}(\boldsymbol{k}+ \ i \mid \boldsymbol{k}) \leq \boldsymbol{y}_{ub} \\ & \forall i \in \{N_1, \cdots, N_2\} \text{and} j \in \{(0, \cdots, N_u\}. \end{aligned}$$

We will refer to the predicted state k + i at time point k as x(k + i|k). Bold written variables indicate higher dimensions, i.e. a vector (lowercase characters) or a matrix (uppercase characters). A sequence of states will be indicated by x(·) [5]:

$$\begin{aligned} \boldsymbol{x}(\boldsymbol{k}+i) \quad & \forall i \in (0, \cdots, N_2) \Rightarrow \boldsymbol{x}(\cdot), \\ \boldsymbol{u}(\boldsymbol{k}+i) \quad & \forall i \in (0, \cdots, N_u) \Rightarrow \boldsymbol{u}(\cdot), \\ \boldsymbol{y}(\boldsymbol{k}+i) \quad & \forall i \in (N_1, \cdots, N_2) \Rightarrow \boldsymbol{y}(\cdot). \end{aligned}$$

In this way, the constraint formulation will be abbreviated by:

$$\boldsymbol{x}_{lb} \leq \boldsymbol{x}(\cdot) \leq \boldsymbol{x}_{ub} \Rightarrow \boldsymbol{x} \in \mathbb{X}_f,$$

indicating that the sequence x(·) is in the feasible set Xf.

For the MPC designer to generate the optimization problem or cost function, we set the parameters, give the state-space plant model and generate the MPC object as in the following MATLAB script:

```
%Buck Converter model parameters

L = 400e-6;          %Inductor inductance (henry)
Cx = 100e-6;          %Capacitor capacitance (farad)
Vin = 400;           %Input voltage (volts)
```

```
Ro = 50;              %Rated load resistance (ohm)
Verr = 0.05;          %Input Voltage Error (%)
f_err = 20;           %Error frequency (Hz)
f_sw = 100e3;           %Switching frequency (Hz)

%State Space Definition
A = [0 -1/L; 1/Cx -1/(Ro*Cx)];
B = [Vin/L; 0];
C = [0 1];
D = 0;
system = ss(A,B,C,D);

%MPC Object creation
Ts = 0.1e-03;     %Sampling time of the system
p = 15;          %Prediction Horizon value
m = 5;           %Control Horizon Value

MV = struct('Min',0,'Max',1);        %Defining the MV - u(t) - duty cycle Constraints
OV = struct('Min',0, 'Max',400);     %Defining Measured Output Variable Constraints
W = struct('MV',1,'OV',0.1);        %Defining the MV and the OV Weights

mpc1_1_C =  mpc(system, Ts, p, m, W, MV, OV);
mpc1_1_C.Model.Plant.OutputName = {'Voltage'};
mpc1_1_C.Model.Plant.OutputUnit = {'Volts'};
mpc1_1_C.Model.Plant.InputName = {'Duty Cycle'};
```

The parameters of the MPC are described as:

- Sample Time [Ts]:
Rate at which the controller executes the Control Algorithm.

- Prediction Horizon [p]:
Number of predicted future time steps.

- Control Horizon [m]:
From the set of future control actions leading to the predicted plant output, the control horizon is the number of control moves per time step, each control move can be thought of as a free variable that needs to be computed by the optimizer. Usually the first control moves have a significant effect on the predicted output behaviour, and the rest a minor effect, therefore choosing a really high control horizon only increases computational effort.

-Constraints [MV,OV]:
MPC can incorporate constraints and rate of change constraints to the inputs and outputs of the plant, these can be soft or hard.

-Weights [W]:
Give the rate of importance to the input and/or output relative to the expectancy of the user (Could be set to reach the economically desirable steady state value).

As we simulate the plant and MPC model with the parasitic error generator for the plant the simulink model was created:

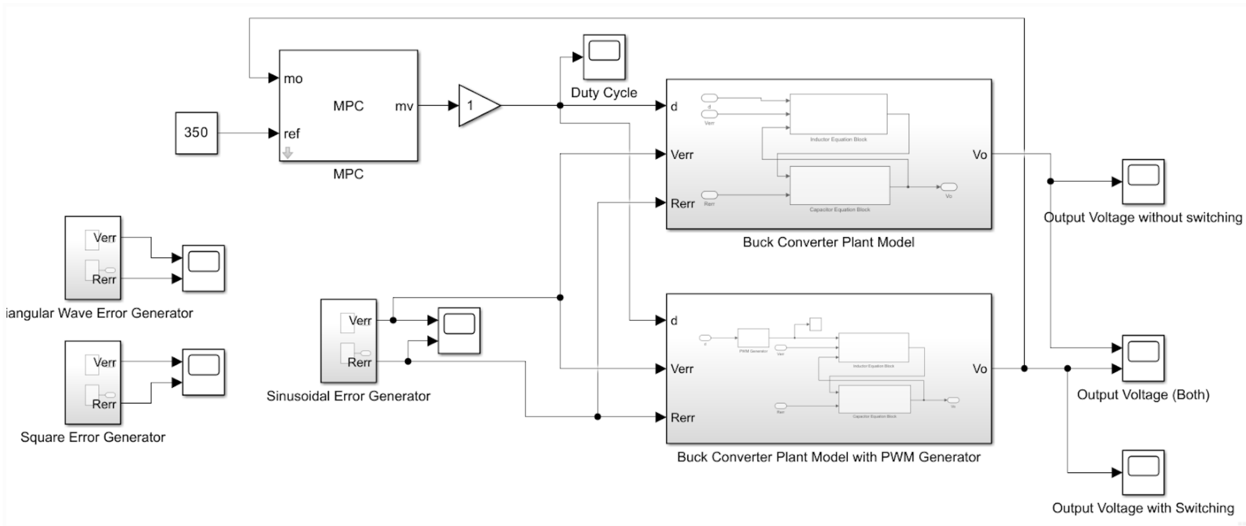

Figure 13. Simulink MPC DC-DC Converter model

4. Simulation Result

4.1. Buck Converter with Square Wave Disturbances on *Vin* and *Ro*

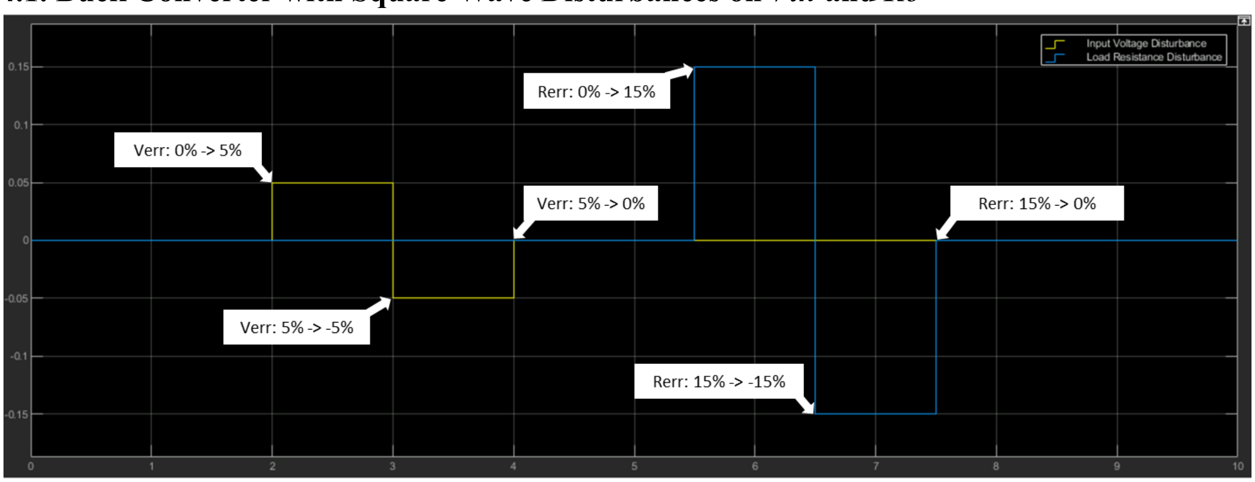

Figure 14. Square Wave Disturbances Applied in the Simulation

Figure 14 shows the applied disturbance for this simulation. These disturbances simulate unideal conditions likely to occur in the buck converter operation for EV charger application. The value of *Verr* simulates the input voltage rise or drop from the rectifier and *Rerr* represents the changes in battery internal resistance. Inability to compensate for these disturbances can harm the battery during charging. For this simulation, the deviation of 5% in the buck converter input voltage is applied at t=2 and it's forced to be this value for 1 second. At t=3, the disturbances drop from 5% to -5% until t=4 when the input voltage has not undergone the disturbances. Similar pattern applied for the disturbances on the load resistance with different timing and deviation (15% and -15%).

➔ Simulation Results using Buck Converter Plant without Switching Operation

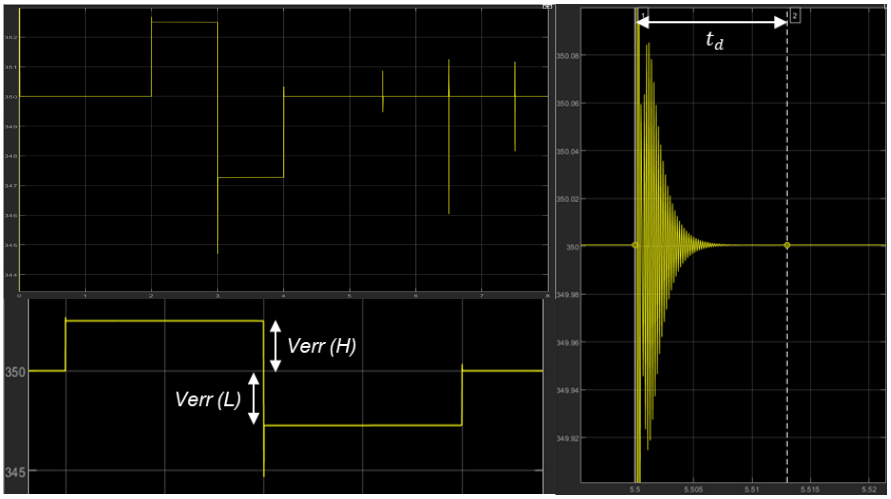

Figure 15. (a) Square Wave Simulation Result without Switching (top left), (b) definition of voltage deviation Verr (bottom left), (c) definition of transient settling time td (right)

Typical simulation result of buck converter with MPC controller and neglecting switching operation is shown in *Figure 15(a)*. It is shown that after disturbances on input voltage applied, MPC controllers are unable to bring down the output voltage to its desired value (350V). It is caused because disturbances occur in the term coupled with the input *d* in the state space (16) so MPC controllers have difficulties in compensating with the error, unless it is specified in the MPC controller implementation. However, MPC controllers have compensated the 20V (5% of 400V) disturbances to a small number of *Verr* as shown in *Figure 15(b)*. On the other hand, MPC can handle the disturbance on the load resistance very well with the transient settling time *td* shown in *Figure 15(c)*. Transient settling time *td* is defined as time required for MPC to compensate for load resistance disturbance until the ripples stay within 0.1Vpp. In this work, the effect of MPC parameters *Ts*(sampling time), *Np*(Prediction Horizon), *Nc*(Control Horizon), *Q*(Output Weight), and *R*(Input Weight) to *Verr* and *td* is observed. For scenario 6 to 8, duty cycle deviation *pdc* during *Vin* and *Ro* disturbances from its value in equilibrium (0.875) is also measured to see the effect of changing the input and output weights on the MPC controller performance. The summary of the simulation results is presented in the following table.

Scenario	MPC Parameters					Simulation Result					
	Ts	Np	Nc	Q	R	Verr(H)	Verr(L)	td(H)	td(L)	pdc(Vin)	pdc(Ro)
1	0.1mS	15	5	350	0.1	2.5V	-2.7V	2mS	2.9mS	-	-

2	0.1mS	50	5	350	0.1	2.5V	-2.7V	2mS	2.9mS	-	-
3	0.1mS	15	13	350	0.1	2.2V	-2.4V	3.9mS	4.3mS	-	-
4	0.01mS	15	5	350	0.1	0.12V	-0.13V	30uS	51.5uS	-	-
5	1mS	15	5	350	0.1	14V	-13.6V	-	-	-	-
6	0.1mS	15	5	0.1	1	2.86V	-3.11V	4.15 mS	5.95mS	0.035	0.076
7	0.1mS	15	5	1	1	2.5V	-2.73V	4.75mS	7.750mS	0.035	0.125
8	0.1mS	15	5	10	0.1	2.5V	-2.73V	4.75mS	7.750mS	0.035	0.125

Table 2. Summary of the Simulation Result with Different MPC Parameters (neglecting the switching operation)
H: disturbance goes from 0% to 5/15%, L: disturbance goes from 5/15% to -5/15%

From scenario 1,2 and 3, it is understood that increasing the prediction horizon does not improve the buck converter performance necessarily during disturbances occurring on input voltage and load resistance. Also, increasing the control horizon close to the prediction horizon can improve the performance slightly although it will add small ripples during the occurrence of input voltage disturbance.

Scenario 4 and 5 shows the effect of increasing and decreasing the sampling time of MPC to the buck converter performance. Decreasing the sampling time or increasing the sampling frequency will greatly improve the performance, as it increases the accuracy of the MPC controller. Conversely, increasing the sampling time or decreasing the sampling frequency will greatly harm the performance of the buck converter during the occurrence of disturbances. It will also affect the buck converter performance during normal operation as it generates a considerable amount of ripples as shown in *Figure 16*.

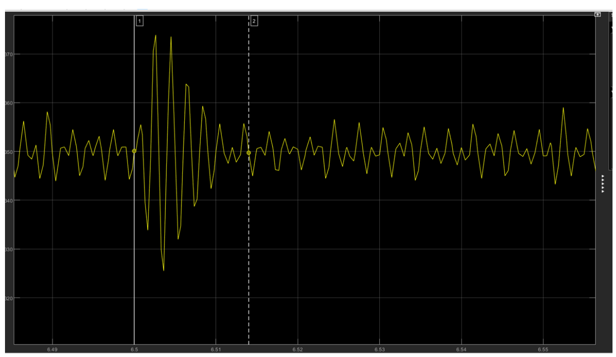

Figure 16. 11-14V Ripples when Sampling Time = 1mS

Scenario 6,7 and 8 exhibit the effect of output and input weights to buck converter performance. Increasing the output weight and input weight ratio (*Q/R*) can reduce output voltage deviation *Verr* during disturbance on input voltage, but it will increase the transient settling time *td*. However, reducing *Q/R* ratio only gives positive improvements on duty cycle deviation during *Ro* disturbance.

➔ Simulation Results using Buck Converter Plant with Switching Operation

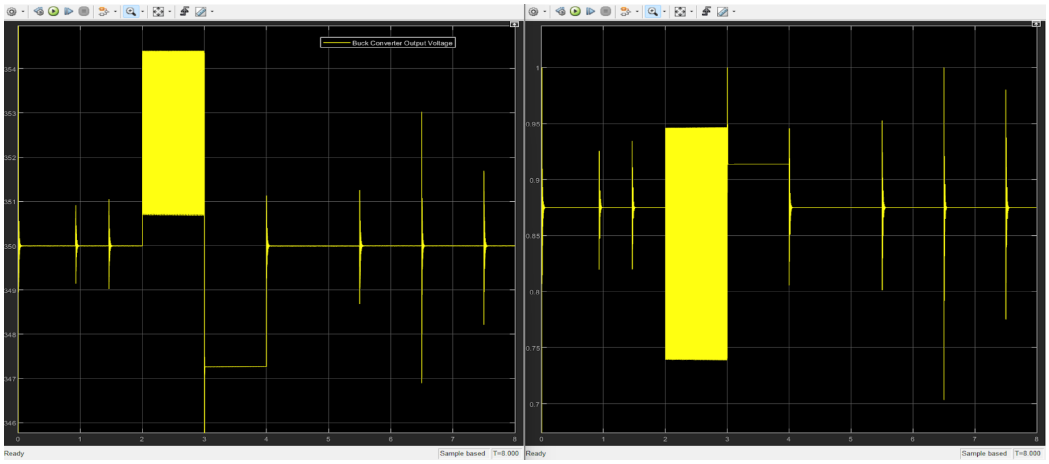

Figure 17 (a) Measured Output voltage with switching operation (left). (b) Measured MV Input Duty cycle (right).

In the previous *Figure 17(a)* and *(b)* it is appreciated how the transients and harmonic distortion is introduced relative to the switching frequency and in comparison to the simulation without the switching there is greater transients and slower settling time, as the sampling time (Ts) of the MPC and the frequency of operation of the plant do not coincide.

Scenario	MPC Parameters						Simulation Result			
	Ts	f_sw	Np	Nc	Q	R	Verr(H)	td(Ro)	dc(Vin)	pdc(Ro)
1	0.1mS	100kHz	15	5	350	0.1	0.7-4.3Vr	32mS	-	-
2	0.1mS	100kHz	50	5	350	0.1	0.7-4.3Vr	26mS	-	-
3	0.1mS	100kHz	15	13	350	0.1	0.6-4.6Vr	-	-	-
4	0.01mS	100kHz	15	5	350	0.1	.09V	168us	-	-
5	10mS	100kHz	15	5	350	0.1	11V	40mS	-	-
6	0.1mS	100kHz	15	5	0.1	1	2.85V	2.1mS	0.034	0.12
7	0.1mS	100kHz	15	5	1	1	0.7-4.3Vr	32mS	0.17-0.19	0.12
8	0.1mS	100kHz	15	5	10	0.1	0.7-4.3Vr	25mS	0.16-.2	0.12

Table 3. Summary of the Simulation Result with Different MPC Parameters (with the switching operation)
H: disturbance goes from 0% to 5/15%, L: disturbance goes from 5/15% to -5/15%

From *Table 3*, it can be deduced that from Scenario 1 to 2 there also isn't a major change, only the settling time for the parasitic resistance is slightly better for a bigger prediction horizon. For the 3rd Scenario when the control horizon is closer to the prediction horizon, the user may be able to see the voltage ripple difference for the Verr, but for the Rerr a very high frequency transient of voltage is introduced and it makes the resistance error not readable, as shown in the following figure.

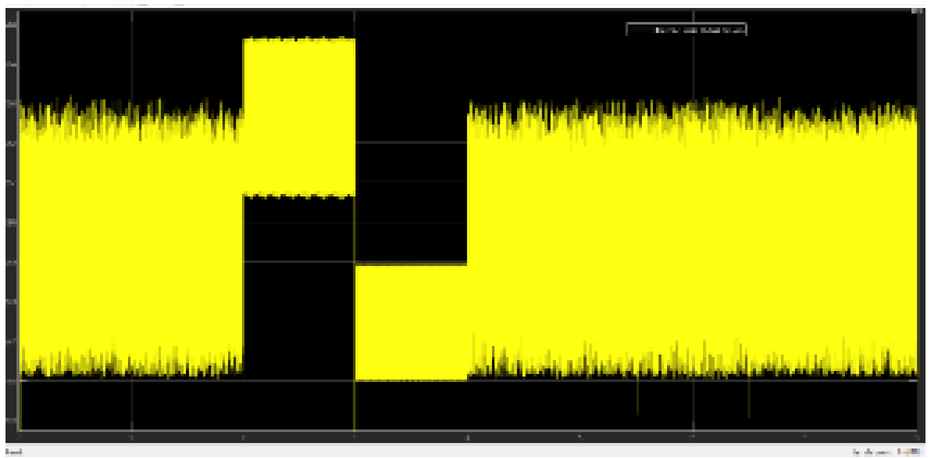

Figure 18 Simulation Results with a very high frequency ripple.

In the 4th Scenario, the transients are highly reduced and the Verr is reduced up until .09V peak, also the Rerr is highly reduced making it almost unreadable, nevertheless there exists a very low voltage error, which has a very fast settling time of almost 168 us.

From the Scenarios 6,7 and 8 we evaluate the MPC performance with the change of weights and how this impacts the output voltage and the duty cycle itself and we are able to conclude that if the weight of the input is higher than the weight of the output, it makes the delta change of the duty cycle smaller, but at the cost of a delay or shift of the measured output, because in that case the Measured output steady state value had a .2 lower shift.

4.2.Buck Converter with Sinusoidal Wave Disturbances on *Vin* and *Ro*

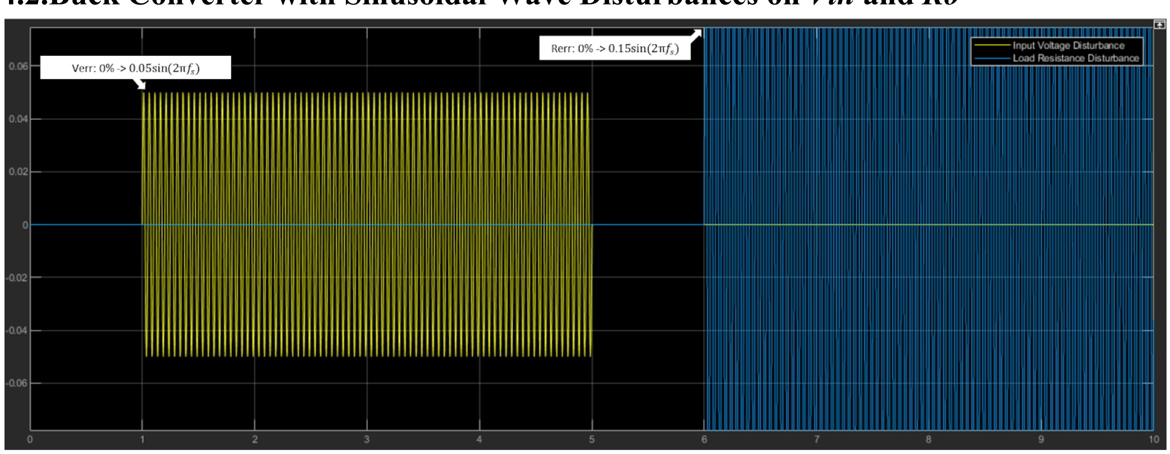

Figure 19. Sinusoidal Wave Disturbances Applied in the Simulation

To simulate the effect of total harmonic distortion in the input voltage and the load resistance, sinusoidal wave error is applied to the buck converter plant for this case. Sinusoidal wave of *Verr* with the amplitude of 0.05 (5%) is applied from t =1 until t=5. At t=6, sinusoidal wave error of load resistance *Rerr* with amplitude of 0.15 (15%) is fed to the plant. The MPC performance with given error frequency f_s is being observed in this work.

➔ Simulation Results using Buck Converter Plant without Switching Operation

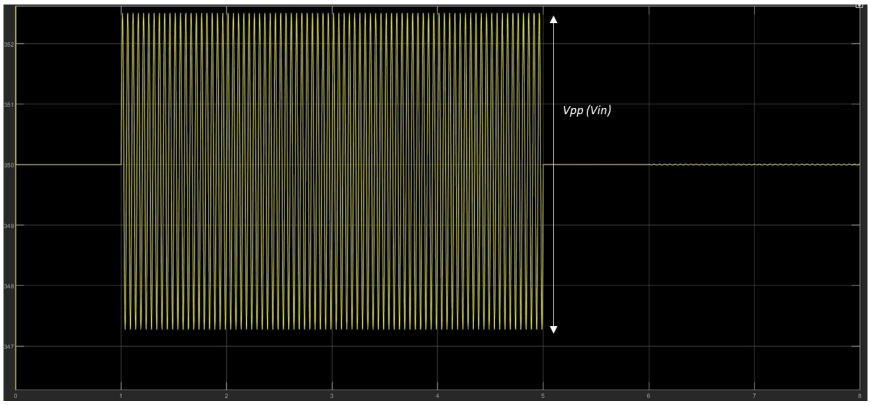

Figure 20. Sinusoidal Wave Disturbances with Frequency = 20Hz Applied in the Simulation

Sinusoidal wave disturbances on input voltage and load resistance will cause sinusoidal ripples in the converter output as shown in *Figure 20*. The peak-to-peak voltage of the ripples *Vpp* caused by disturbances on *Vin* and *Ro* is measured and compared with the MPC parameters such as *Ts*(sampling time), *Np*(Prediction Horizon), *Nc*(Control Horizon), *Q*(Output Weight), and *R*(Input Weight) to observe the effect of these MPC parameters and the converter performance. For scenario 5 to 7, duty cycle deviation *pdc* during *Vin* and *Ro* disturbances from its value in equilibrium (0.875) is also measured to see the effect of changing the input and output weights on the MPC controller performance. The summary of the simulation results is presented in the following table.

Scenario	**MPC Parameters**						**Simulation Result**			
	Ts	**f_err**	**Np**	**Nc**	**Q**	**R**	**Vpp(Vin)**	**Vpp(Ro)**	**pdc(Vin)**	**pdc(Ro)**
1	0.1mS	20Hz	15	5	350	0.1	5.2V	0.016V	-	-
2	0.1mS	20Hz	50	5	350	0.1	5.2V	0.016V	-	-
3	0.1mS	20Hz	15	13	350	0.1	4.58V	0.014V	-	-
4	0.01mS	20kHz	15	13	350	0.1	0.36V	0.7V	-	-
							0.31V	0.013V	-	-
5	0.1mS	20Hz	15	5	0.1	1	5.9V	0.18V	0.072	2.20E-04
6	0.1mS	20Hz	15	5	1	1	5.23V	0.016V	0.074	2.34E-04
7	0.1mS	20Hz	15	5	10	0.1	2.83V	0.018V	0.072	2.20E-04

Table 4. Summary of the Simulation Result with Different MPC Parameters (neglecting the switching operation) using Sinusoidal Wave Error

Similar to the behaviour when square wave disturbance is applied, increasing the prediction horizon does not improve the performance while increasing control horizon can improve the performance slightly. Also, reducing the sampling time of the MPC or increasing the frequency will enhance the performance massively as shown in scenario 3. For scenario 5 to 7, it showed that increasing the output weight and input weight ratio (*Q/R*) can improve performance during *Vin* disturbance while reducing the input weight

From scenario 4, it can be recognized that the MPC controller performs better when the error frequency is high. In this case, instead of sinusoidal wave error in the output voltage, the output voltage attenuates from the moment disturbance started until the ripples are small as shown in *Figure 21*. Hence, the maximum and minimum *Vpp* values are measured only for scenario 4.

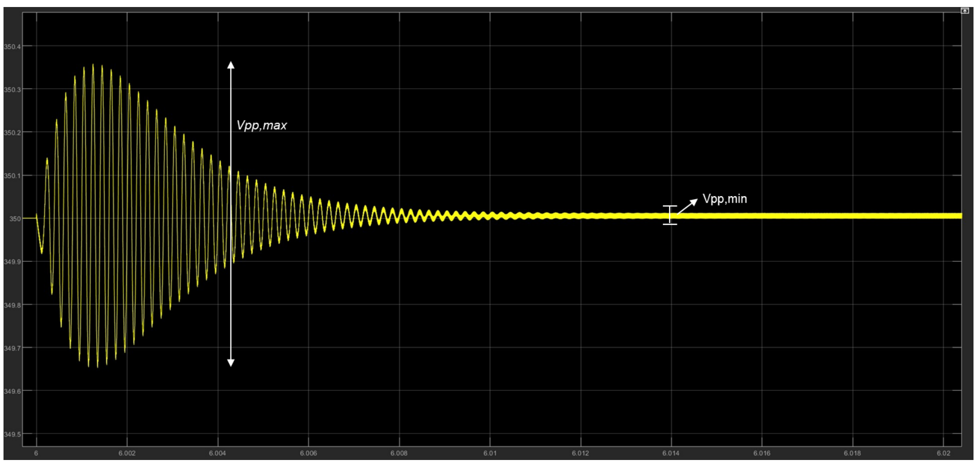

Figure 21. Output Voltage when frequency error 20kHz

➔ Simulation Results using Buck Converter Plant with Switching Operation

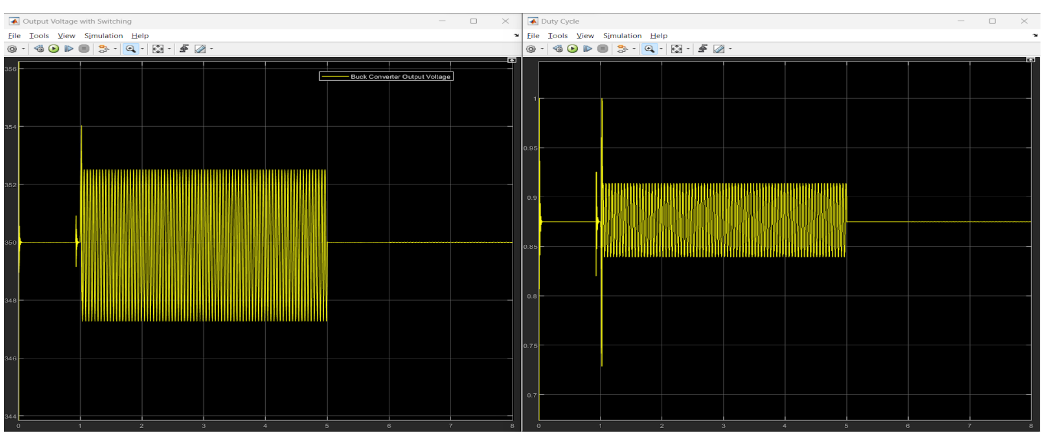

Figure 22. Measured Output Voltage(left) and Duty Cycle(right)

As seen in the previous figure, the introduction of more harmonics and transients in the case of the simulation with different frequency for the switching is present. The following table shows the results for all the possible scenarios for the Sine wave parasitic error with the different switching frequency *f_sw* = 100khz.

Scenario	**MPC Parameters**						**Simulation Result**			
	Ts	**f_err**	**Np**	**Nc**	**Q**	**R**	**T(Vin)**	**T(Ro)**	**pdc(Vin)**	**pdc(Ro)**
1	0.1mS	20Hz	15	5	350	0.1	52.5mS	51mS	-	-
2	0.1mS	20Hz	50	5	350	0.1	50mS	49mS	-	-
3	0.1mS	20Hz	15	13	350	0.1	50mS	-	-	-
4	0.1mS	20kHz	15	5	350	0.1	-	-	-	-
5	0.1mS	20Hz	15	5	0.1	1	50mS	50mS	0.072	0.0002
6	0.1mS	20Hz	15	5	1	1	50mS	50mS	0.072	0.0002
7	0.1mS	20Hz	15	5	10	0.1	50mS	50mS	0.074	0.0002

Table 5. Summary of the Simulation Result with Different MPC Parameters (with switching operation) using Sinusoidal Wave Error

As previously stated for the other cases, the change in prediction horizon does not make a significant change in the outcome for the MV or the OV, but for the 3rd scenario there is a major change in the settling time when the control horizon is also near prediction horizon, in this case, for the steady state of the system, it presents high frequency transients which also are at the same voltage level of the Rerr as shown in *Figure 23*. Then for the Scenario 4, which presents the increase of the frequency error, there are high frequency transients present at all times, and harmonics in some regions as well.

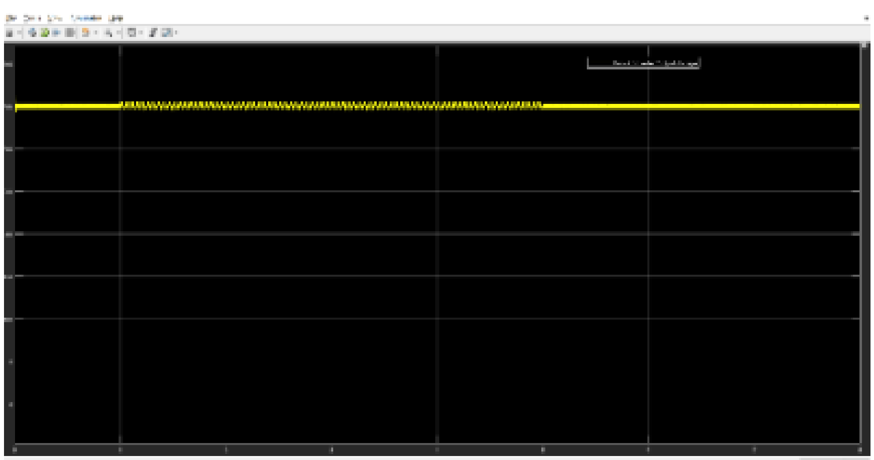

Figure 22. Output Voltage for Scenario 3.

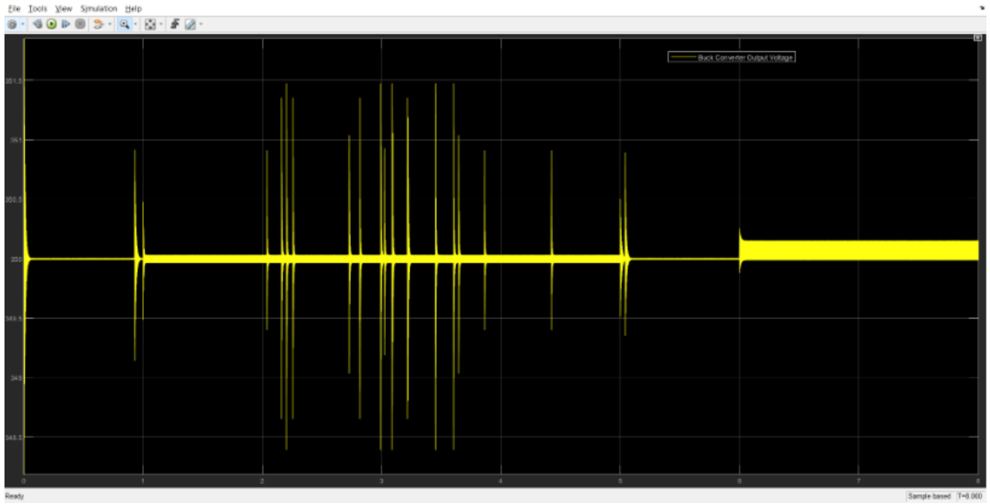

Figure 23. Output Voltage for Scenario 4.

To finalise with the simulation results, for the last 3 Scenarios the measurements didn't change as it is with the different weights, though for the Scenario with bigger weight for the input to the plant there is a .2 shift phase again on the output with the ref value. The behaviour is shown in the following *Figure 24*(a), *(b)* and *(c)*.

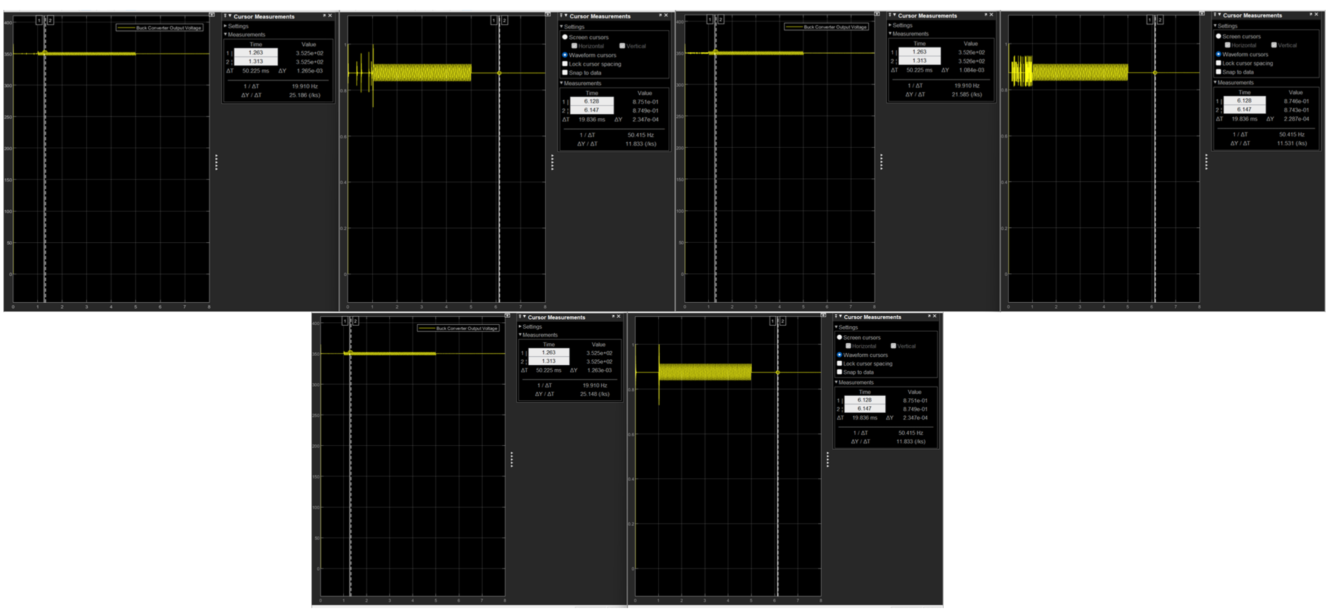

Figure 24. (a) Output Voltage and duty cycle with Weights [1MV-0.1 MO]. (b) Output Voltage and duty cycle with Weights [1MV-1 MO]. (c) Output Voltage and duty cycle with Weights [0.1MV-10 MO].

5. Conclusion

The subject of this work is to evaluate the performance of an MPC controller for DC-DC buck converter with disturbances on the input voltage and the load resistance and to observe the effect of the MPC parameters on the performance. From this work, we can conclude that:

- Linear MPC are not able to regulate the disturbances on the input voltage but it performs well during disturbances on the load resistance.
- Increasing the prediction horizon does not have any effect in reducing the deviation of output voltage when disturbances happen, while increasing the control horizon close to the prediction horizon slightly improves the performance.
- MPC sampling time heavily increases the accuracy of the controller and increasing it will enhance the performance greatly with the downside of increasing computational time.
- Increasing the ratio of output weight and input weight can reduce the output voltage error but it will apply more energy to the system.
- MPC can handle high frequency error to the system and it means it can handle the total harmonic distortion in the input voltage.
- Non-linear MP

References

[1] "Global EV Outlook 2022 – Analysis," *IEA*. https://www.iea.org/reports/global-ev-outlook-2022 (accessed Dec. 29, 2022).

[2] M. Safayatullah, M. T. Elrais, S. Ghosh, R. Rezaii, and I. Batarseh, "A Comprehensive Review of Power Converter Topologies and Control Methods for Electric Vehicle Fast Charging Applications," *IEEE Access*, vol. 10, pp. 40753–40793, 2022, doi: 10.1109/ACCESS.2022.3166935.

[3] S. Vazquez, J. Rodriguez, M. Rivera, L. G. Franquelo, and M. Norambuena, "Model Predictive Control for Power Converters and Drives: Advances and Trends," *IEEE Transactions on Industrial Electronics*, vol. 64, no. 2, pp. 935–947, Feb. 2017, doi: 10.1109/TIE.2016.2625238.

[4] R. W. Erickson and D. Maksimović, *Fundamentals of Power Electronics*. Cham: Springer International Publishing, 2020. doi: 10.1007/978-3-030-43881-4.

[5] M. Schwenzer, M. Ay, T. Bergs, and D. Abel, "Review on model predictive control: an engineering perspective," *Int J Adv Manuf Technol*, vol. 117, no. 5–6, pp. 1327–1349, Nov. 2021, doi: 10.1007/s00170-021-07682-3.

[6] "Tutorial overview of model predictive control," *IEEE Control Syst.*, vol. 20, no. 3, pp. 38–52, Jun. 2000, doi: 10.1109/37.845037.

[7] J. Richalet, A. Rault, J. L. Testud, and J. Papon, "Model predictive heuristic control," *Automatica*, vol. 14, no. 5, pp. 413–428, Sep. 1978, doi: 10.1016/0005-1098(78)90001-8.